

First-Principles Calculations of Electronic States and Self-Doping Effects at a 45° Grain Boundary in the High Temperature YBa₂Cu₃O₇ Superconductor

U. Schwingenschlögl^{1,2} and C. Schuster¹

¹*Institut für Physik, Universität Augsburg, 86135 Augsburg, Germany,*

²*KAUST, PCSE Division, P.O. Box 55455, Jeddah 21534, Saudi Arabia*

(Received 21 February 2009; published 3 June 2009)

The charge redistribution at grain boundaries determines the applicability of high- T_c superconductors in electronic devices because the transport across the grains can be hindered considerably. We investigate the local charge transfer and the modification of the electronic states in the vicinity of the grain-grain interface by *ab initio* calculations for a (normal-state) 45°-tilted [001] grain boundary in YBa₂Cu₃O₇. Our results explain the suppressed interface transport and the influence of grain boundary doping in a *quantitative* manner, in accordance with the experimental situation. The charge redistribution is found to be strongly inhomogeneous, which has a substantial effect on transport properties since it gives rise to a self-doping of 0.10 ± 0.02 holes per Cu atom.

DOI: 10.1103/PhysRevLett.102.227002

PACS numbers: 74.81.Bd, 73.20.-r, 74.25.Jb, 85.25.Am

Electronic transport in wires and tapes from high- T_c compounds is seriously suppressed by structural defects and interfaces. In particular, grain boundaries have been identified as the main limiting factor, which determines the critical current in bulk samples [1]. Grain boundaries in YBa₂Cu₃O_{7- δ} (YBCO) seem to be depleted of charge carriers [2,3]. For this reason, the supercurrent density can be enhanced by locally overdoping the superconductor (by Ca substitution) close to grain boundaries while keeping the grains optimally doped [4]. The overdoping prevents a reduction of the critical temperature [5], which indicates that suppression of the critical current at grain boundaries is connected to interface charging and/or distortions of the local electronic band structure. The latter would also explain that a perovskite superconductor behaves different from conventional or intermetallic superconductors, like MgB₂, where the supercurrent density is hardly affected [6]. Yet, there is evidence for Josephson junction-type weak link grain boundaries in MgB₂ [7].

In perovskite superconductors, the critical current can drop down to 1% of the bulk value for a misorientation angle of 10° [8–10]. For technological applications, optimization of low angle grain boundaries is mandatory and, therefore, addressed by various groups [11–13]. Large angle grain boundaries, on the other hand, are of practical interest as they form excellent Josephson junctions. Using bicrystal substrates or the biepitaxial principle, based on two different substrates, 45° tilted [001] grain boundaries can be grown with a high accuracy [14,15]. Because substrate effects can be eliminated from transport measurements [16], such Josephson junctions are widely used to gain insight into the superconducting state (e.g., the properties and symmetry of the gap function, *s* wave versus *d* wave) [15,17]. In addition, mesoscopic fluctuations of the magnetoconductance point to a coexistence of supercurrent and quasiparticle current [18].

It is surprising that a first-principles electronic structure calculation, which can account for structural details at grain boundaries, is missing so far. Probably, this fact is connected to a tremendous demand on CPU time. For the simpler Ti-based perovskite insulators SrTiO₃ and BaTiO₃, two common substrates for YBCO, analogous studies of grain boundaries have been performed by Klie *et al.* [19], using the Thomas-Fermi screening approach, as well as by Imaeda *et al.* [20], using density functional theory (DFT). Moreover, superconductor-metal interfaces, which are closely related to grain boundaries in high- T_c materials [21,22], have been addressed by DFT calculations. For YBCO-Pd interfaces, as a prototypical example, a net charge transfer of ~ 0.1 holes per Cu atom off the CuO₂ planes has been established [23], showing only a weak dependence on the interface orientation [24].

Contrary to conventional superconductors, bending of the band structure by a variation in the charge distribution is strong enough to control the transport in high- T_c compounds [14] because of large dielectric constants and small carrier densities [25]. The Thomas-Fermi screening length (over which a band-bending is effective) therefore grows to the order of magnitude of the superconducting coherence length. Consequently, the technical optimization of grain boundaries calls for further insight into the local electronic structure. This issue is addressed in the present Letter for a 45°-tilted [001] grain boundary. Since the electronic states are expected to depend strongly on the local atomic environment, we use the DFT approach to obtain and study a fully relaxed YBCO grain boundary in a supercell of altogether 317 atoms. Our data provide evidence for a characteristic charge transfer between the CuO₂ chains and CuO chains. We explain this effect in terms of the modifications of the chemical bonding.

Our results are based on density functional theory and the generalized gradient approximation, as implemented in

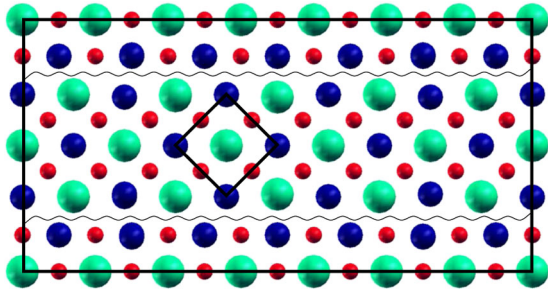


FIG. 1 (color online). Structural setup used for simulating a 45° YBCO grain boundary (wiggly line), in a projection along the YBCO c axis. Large spheres represent Y/Ba, medium spheres Cu, and small spheres O. Whereas the square highlights a YBCO unit cell, the outer rectangle indicates the boundaries of the supercell.

the WIEN2K package [26]. By its all-electron scheme, this full-potential linearized augmented-plane-wave code is suitable for dealing with structural relaxation and the induced charge redistribution in complex geometries, applying a supercell approach [27]. From a technical point of view, the electronic states at YBCO grain boundaries are accessible to the supercell approach, based on three-dimensional periodic boundary conditions, since relevant effects are proposed to take place on the length scale of the lattice constant. Typical experimental screening lengths for doped YBCO systems are ~ 4.5 Å [28], which is an upper limit for the system under investigation. A supercell therefore can cover the essentials of the electronic interaction if density functional theory predicts the correct screening length.

The supercell which we use for simulating a 45° -tilted [001] grain boundary is displayed in Fig. 1, in a projection parallel to the c axis of the parent YBCO unit cell (black square). Our structural setup reduces the number of atomic sites entering the calculation to the necessary minimum. A further reduction is not possible since one would not maintain both Cu and O atoms in a bulklike coordination. We mention that a (minor) lattice strain is present in our supercell by construction. It results from a lattice mismatch of less than 1% of the YBCO lattice constants between the

neighboring grains in our supercell: five 45° -tilted and seven nontilted YBCO unit cells form the grain boundary, compare Fig. 1. The strain has to be accepted in order to keep periodic boundary conditions. However, the mismatch is small enough to ensure that there is no drawback on the validity of our results. For sampling the Brillouin zone a $5 \times 5 \times 2$ mesh with 25 points in the irreducible wedge is applied. We use 2502 local orbitals and about 840 000 plane waves to represent the charge density. The cutoff is set to $RK_{\max} = 4$.

Turning to the results of our electronic structure calculations for the YBCO grain boundary, we give in Fig. 2 an overview of the valence states, consisting of the Cu $3d$ and O $2p$ orbitals. The DOS curves which we present here and in the following are normalized by the number of contributing atoms in order to simplify a comparison. The Cu $3d$ DOS exhibits a broad structure with one pronounced maximum centered at about -2 eV. This shape reflects the YBCO bulk data except for the fact that the width of the -2 eV peak is increased, which is expected since the different Cu atoms at a disordered grain boundary should have slightly different chemical surroundings. Likewise, similar to bulk YBCO, there are substantial O $2p$ contributions in the entire Cu $3d$ energy range up to the Fermi level due to a strong Cu-O hybridization. The latter also explains the Cu $3d$ admixtures at low energy. However, at this point, we encounter an important difference to bulk YBCO [29]: A distinct portion of electronic states appears below -7 eV. These states, of course, are related to the modified bonding at the grain boundary.

In order to analyze the Cu-O bonding in more detail, the DOS can be projected on the atomic sites of interest. Corresponding results are given in Fig. 2. In the central panel, we compare the O $2p$ DOS of two (representative) bulklike O atoms, one from a BaO layer and one from a CuO chain. The term “bulklike” is used to indicate that an atom is coordinated as in bulk YBCO; i.e., its first coordination sphere is not affected by the grain boundary. For all bulklike O atoms, we obtain a similar behavior: Above some -5 eV, the DOS resembles the bulk YBCO DOS, whereas two additional peaks appear at lower energy. These states trace back to additional CuO bonds created

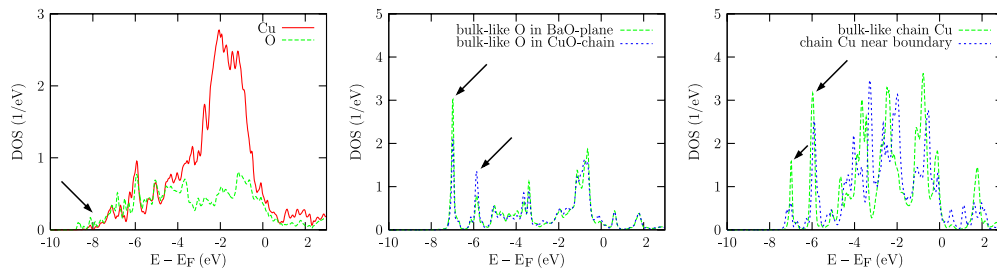


FIG. 2 (color online). Left: partial Cu $3d$ and O $2p$ DOS for the entire supercell, normalized by the number of Cu/O atoms. Center/right: site-projected DOS of selected sites in the 45° YBCO grain boundary: bulklike coordinated O (center; showing two examples) and Cu at the grain boundary compared to bulklike coordinated Cu (right; both on CuO chain sites).

at the grain boundary due to the broken translational symmetry, see Fig. 1. Yet, because they reappear for bulklike atoms, they cannot be described in terms of localized states at the grain-grain interface. A possible explanation would be a substantial delocalization of the hybridized Cu-O states, which could reach deep into the grain. However, our minimal supercell does not allow us to resolve the latter. In contrast to the naive expectation for d electron orbitals, such a delocalization seems to be typical for metallic YBCO [30]. This line of reasoning is supported by the Cu $3d$ DOS. On the right hand side of Fig. 2, we show, as a representative example, data for Cu atoms from a CuO chain. Both for the bulklike and the boundary atom, the new low energy states are present.

It is well established that the electronic characteristics of copper oxides depend severely on details of the chemical bonding and on the doping [31,32]. Here, our results show an interdependence between the modified chemical bonding at the grain boundary and the charge distribution between the structural building blocks, in particular, the CuO₂ planes and CuO chains. While the creation of additional CuO bonds predominantly affects the low energy range of the valence states, see the previous discussion, Fig. 3 demonstrates that there are likewise distinct alterations at the Fermi energy (E_F). For selected bulklike atoms in our supercell, i.e., Cu in the CuO₂ planes (left top) and in the CuO chains (left bottom), Y (right top), and Ba (right bottom), we study the site-projected DOS for the grain boundary (dashed line) in comparison to the respective bulk YBCO results (solid line). Around E_F , we find significant shifts of the energetic positions of the band edges, indicated by arrows in Fig. 3.

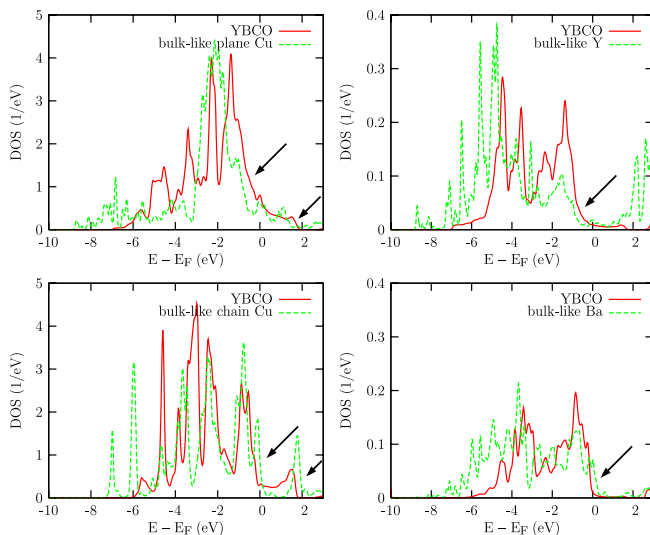


FIG. 3 (color online). Partial (site-projected) DOS of selected bulklike coordinated atoms in the 45° YBCO grain boundary, as compared to the corresponding YBCO bulk DOS: Cu in the CuO₂ planes (left top), Cu in the CuO chains (left bottom), Y (right top), and Ba (right bottom).

For the CuO₂ planes, the electronic states shift to the low energy side. The electron count hence increases near the grain boundary; i.e., the hole count is reduced. Quantitative evaluation yields a reduction of 0.10 ± 0.02 holes per Cu atom, which is a substantial modification of the local doping state and should be accompanied by strong changes in the electronic properties of the CuO₂ planes. With reference to the YBCO phase diagram [33], it is to be expected that this hole underdoping will prohibit the transition of the grain boundary into a superconducting state. The shift of the electronic states can also be interpreted as a compactification of the Cu $3d$ DOS for sites at a grain boundary, see the left top panel of Fig. 3. This corresponds to a reduced delocalization of the hybridized Cu-O states, tracing back to the broken lattice periodicity. Hence, we attribute the charge transfer towards the CuO₂ planes to an enhanced spatial localization of the near- E_F Cu-O states. Finally, the additional charge originates from the CuO chains, see the left bottom panel of Fig. 3, since here the band edges shift in the opposite direction, i.e., to higher energy. Because of the small portion of Y and Ba contributions to the valence states, these sites play a minor role for the redistribution. The hole density in the CuO₂ planes is shown in Fig. 4 by contour plots for the area of the square in Fig. 1. The observed hole reduction affects almost the entire CuO₂ plane to a similar degree, where qualitative deviations of the contours appear only perpendicular to the grain boundary.

In conclusion, we have studied a 45°-tilted [001] grain boundary in YBCO by density functional theory and performed a full structure optimization. As to be expected, we obtain significant modifications of the CuO chemical bonding due to additional combinations of effective overlap between Cu $3d$ and O $2p$ orbitals at the grain-grain interface. Beyond, the bulklike Cu-O states are subject to enhanced localization near the grain boundary as the crystal lattice is perturbed. This results in an energetic shift of the electronic states in the vicinity of the Fermi level,

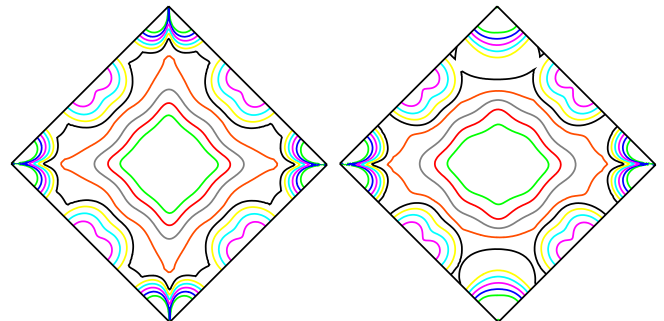


FIG. 4 (color online). Contour plots of the hole density, i.e., the integrated total DOS between the Fermi level and 1.9 eV, in the CuO₂ planes of bulk YBCO (left) and of the supercell (right). The display area is the square shown in Fig. 1, with Cu in the corners and O in the centers of the edges.

which has almost the same amplitude in the CuO_2 planes and the CuO chains, but the opposite sign.

As a consequence, there is a substantial charge transfer between these structural building blocks. The CuO_2 planes are affected by a charge carrier (hole) depletion of 0.10 ± 0.02 holes per Cu atom. A grain boundary, hence, can be interpreted in terms of (intrinsically) underdoped CuO_2 planes, which explains a suppressed transition into a superconducting state. In addition, it explains the fact that the supercurrent density can be enhanced by a local hole overdoping of the grain boundaries [4,5] since this compensates the intrinsic underdoping. Assuming that a third of the additional holes enters the CuO_2 planes, the maximum of the enhancement for 30% Ca doping agrees even quantitatively with the obtained first-principles results. Finally, going beyond experimental data [2,3], the charge redistribution is found to be *inhomogeneous* with depletion and accumulation zones at the grain boundary, while there is little charge transfer to or off the grain. New experiments are indicated to confirm this observation.

We acknowledge fruitful discussions with J. Mannhart as well as financial support by the Deutsche Forschungsgemeinschaft (SFB 484).

-
- [1] D. Dimos, P. Chaudhari, J. Mannhart, and F. K. Legoues, *Phys. Rev. Lett.* **61**, 219 (1988).
- [2] S. E. Babcock, X. Y. Cai, D. C. Larbalestier, D. H. Shin, N. Zhang, H. Zhang, D. L. Kaiser, and Y. Gao, *Physica C (Amsterdam)* **227**, 183 (1994).
- [3] N. D. Browning, M. F. Chisholm, S. J. Pennycook, D. P. Norton, and D. H. Lowndes, *Physica C (Amsterdam)* **212**, 185 (1993).
- [4] A. Schmehl, B. Goetz, R. R. Schultz, C. W. Schneider, H. Bielefeldt, H. Hilgenkamp, and J. Mannhart, *Europhys. Lett.* **47**, 110 (1999).
- [5] G. Hammerl, A. Schmehl, R. R. Schulz, B. Goetz, H. Bielefeldt, C. W. Schneider, H. Hilgenkamp, and J. Mannhart, *Nature (London)* **407**, 162 (2000).
- [6] S. B. Samanta, H. Narayan, A. Gupta, A. V. Narlikar, T. Muranaka, and J. Akimitsu, *Phys. Rev. B* **65**, 092510 (2002).
- [7] N. Khare, D. P. Singh, A. K. Gupta, S. Sen, D. K. Aswal, S. K. Gupta, and L. C. Gupta, *J. Appl. Phys.* **97**, 076103 (2005).
- [8] D. Dimos, P. Chaudhari, and J. Mannhart, *Phys. Rev. B* **41**, 4038 (1990).
- [9] Z. G. Ivanov, P. A. Nilsson, D. Winkler, J. A. Alarco, T. Claeson, E. A. Stepanov, and A. Y. Tzalenchuk, *Appl. Phys. Lett.* **59**, 3030 (1991).
- [10] T. Amrein, L. Schultz, B. Kabius, and K. Urban, *Phys. Rev. B* **51**, 6792 (1995).
- [11] D. T. Verebelyi, D. K. Christen, R. Feenstra, C. Cantoni, A. Goyal, D. F. Lee, M. Paranthaman, P. N. Arendt, R. F. DePaula, J. R. Groves, and C. Prouteau, *Appl. Phys. Lett.* **76**, 1755 (2000).
- [12] J. E. Evetts, *Supercond. Sci. Technol.* **17**, S315 (2004).
- [13] A. Weber, C. W. Schneider, S. Hembacher, C. Schiller, S. Thiel, and J. Mannhart, *Appl. Phys. Lett.* **88**, 132510 (2006).
- [14] H. Hilgenkamp and J. Mannhart, *Rev. Mod. Phys.* **74**, 485 (2002).
- [15] S. K. H. Lam and S. Gnanarajan, *Phys. Rev. B* **78**, 094521 (2008).
- [16] J. H. T. Ransley, P. F. McBrien, G. Burnell, E. J. Tarte, J. E. Evetts, R. R. Schulz, C. W. Schneider, A. Schmehl, H. Bielefeldt, H. Hilgenkamp, and J. Mannhart, *Phys. Rev. B* **70**, 104502 (2004).
- [17] A. Tagliacozzo, D. Born, D. Stornaiuolo, E. Gambale, D. Dalena, F. Lombardi, A. Barone, B. L. Altshuler, and F. Tafuri, *Phys. Rev. B* **75**, 012507 (2007).
- [18] A. Tagliacozzo, F. Tafuri, E. Gambale, B. Jouault, D. Born, P. Lucignano, D. Stornaiuolo, F. Lombardi, A. Barone, and B. L. Altshuler, *Phys. Rev. B* **79**, 024501 (2009).
- [19] R. F. Klie, M. Beleggia, Y. Zhu, J. P. Buban, and N. D. Browning, *Phys. Rev. B* **68**, 214101 (2003).
- [20] M. Imaeda, T. Mizoguchi, Y. Sato, H. S. Lee, S. D. Findlay, N. Shibata, T. Yamamoto, and Y. Ikuhara, *Phys. Rev. B* **78**, 245320 (2008).
- [21] T. Emig, K. Samokhin, and S. Scheidl, *Phys. Rev. B* **56**, 8386 (1997).
- [22] B. K. Nikolic, J. K. Freericks, and P. Miller, *Phys. Rev. B* **65**, 064529 (2002).
- [23] U. Schwingenschlögl and C. Schuster, *Europhys. Lett.* **77**, 37007 (2007); *Phys. Rev. B* **79**, 092505 (2009).
- [24] U. Schwingenschlögl and C. Schuster, *Appl. Phys. Lett.* **90**, 192502 (2007); *J. Appl. Phys.* **102**, 113720 (2007).
- [25] G. A. Samara, W. F. Hammetter, and E. L. Venturini, *Phys. Rev. B* **41**, 8974 (1990).
- [26] P. Blaha, K. Schwarz, G. Madsen, D. Kvasicka, and J. Luitz, *WIEN2k: An Augmented Plane Wave Plus Local Orbitals Program for Calculating Crystal Properties* (Vienna University of Technology, Vienna, 2001).
- [27] U. Schwingenschlögl and C. Schuster, *Europhys. Lett.* **81**, 17007 (2008); *Chem. Phys. Lett.* **449**, 126 (2007).
- [28] J. Mannhart, *Mod. Phys. Lett. B* **6**, 555 (1992).
- [29] H. Krakauer, W. E. Pickett, and R. E. Cohen, *J. Supercond.* **1**, 111 (1988).
- [30] W. M. Temmerman, H. Winter, Z. Szotek, and A. Svane, *Phys. Rev. Lett.* **86**, 2435 (2001).
- [31] A. Filippetti and V. Fiorentini, *Phys. Rev. Lett.* **95**, 086405 (2005).
- [32] U. Schwingenschlögl and C. Schuster, *Phys. Rev. Lett.* **99**, 237206 (2007); *J. Phys. Condens. Matter* **20**, 382201 (2008).
- [33] W. E. Pickett, *Rev. Mod. Phys.* **61**, 433 (1989).